

Synchrotron-radiation photoemission study of Ba on a Si(001)2×1 surface

Chiu-Ping Cheng,* Ie-Hong Hong, and Tun-Wen Pi†

Synchrotron Radiation Research Center, Hsinchu, Taiwan, Republic of China

(Received 11 December 1997; revised manuscript received 22 April 1998)

A synchrotron-radiation photoemission study of Ba deposited on a clean Si(001)2×1 surface at room temperature is presented. Upon Ba adsorption, the maximum drop in work function is about 2.3 eV. At submonolayer coverage, the asymmetric dimers on the surface are preserved. Near to one monolayer, however, they become symmetric. In the meantime, barium silicides start to form, first the monosilicide followed by the disilicide with increasing coverage. The Si 2*p* core-level photoemission spectra clearly exhibit these monosilicide and disilicide components having a surface core-level shift of 1.05 and 1.84 eV, respectively. [S0163-1829(98)11531-X]

The study of the metal-silicon interfaces is important for technological applications and surface physics. Many efforts have been devoted to the alkali-metal (AM) adsorbates,¹⁻⁶ which have demonstrated quite a few interesting phenomena as nonmetal-metal transition and surface dimers reversion. In contrast, little attention has been paid to the alkaline earth metals such as Ba, although the element in many aspects behaves similarly to the AM.⁷ According to the limited reports obtained from various techniques such as x-ray photoelectron spectroscopy (XPS),^{8,9} Auger electron spectroscopy (AES),^{10,11} low-energy electron diffraction (LEED),¹⁰⁻¹² thermal desorption spectroscopy (TDS),^{10,11,13} and metastable-atom deexcitation spectroscopy (MDS),^{10,13} the behaviors of the Ba/Si(001)2×1 interface can be summarized as (i) Ba grown layer by layer, (ii) ionic interaction between the first Ba overlayer and the silicon surface, leading a charge transfer from the former to the latter, (iii) the second overlayer and above having a metallic character, and (iv) no silicide formation at room temperature. The present high-resolution synchrotron radiation photoemission work on a clean Ba/Si(001)2×1 interface found actually that ionic interaction does not occur, and the Ba silicides can be formed at room temperature, as long as the substrate surface is atomically clean. Further, the dimer reversion from an asymmetric orientation to a symmetric orientation at one monolayer (ML) of Ba thickness is demonstrated.

Photoemission experiments were performed at the Synchrotron Radiation Research Center (SRRC) in Hsinchu, Taiwan, Republic of China. The details can be found elsewhere.¹⁴ In short, photoelectrons were collected via an EA125 hemispherical analyzer (OMICRON). The base pressure of the UHV chamber in all measurements is better than 2.5×10^{-11} Torr. An *n*-type, mirror polished, Si(001) single crystal ($\rho = 1 - 10 \Omega \text{ cm}$, *P*) was preoxidized according to the Ishizaka and Shiraki method.¹⁵ The sample is then annealed stepwise in the photoemission chamber up to 875 °C to remove the protected oxide layers. The pressure of evaporating a thoroughly degassed Ba getter (SAES Getters) was always below 8.5×10^{-11} Torr. Figure 1 shows the change of the Ba *MNN* (56 eV) Auger peak-to-peak height with Ba deposition time. Two kinks at 75 and 150 s of deposition time and the change of the line slopes are clearly seen. We

then refer the time of kink as the completion of a layer. The thickness monitor confirms the calibration as well.

Figure 2 presents the change in work function, $\Delta\phi$, as a function of Ba coverage. As can be seen in Fig. 2, $\Delta\phi$ drops rapidly at low coverage and reaches a maximum value of -2.3 eV at 1.2 ML. Upon further exposure $\Delta\phi$ becomes -2.1 eV, and remains at a constant value of -2.2 eV above 2 ML. At here, the system work function becomes 2.7 eV.¹⁶ This value is close to the work function of the metallic bulk Ba, 2.5 eV.¹⁷

The evolution of the valence-band spectra with Ba coverage is illustrated in Fig. 3. As shown in the figure, the clean spectrum exhibits strong emission from the surface dangling-bond, dimer-related, and backbond states at binding energies of 0.5, 2.1, and 3.0 eV, respectively. Among these three states, the Ba adsorbate most affects the dangling-bond state. As a matter of fact, aside from the reduction of its intensity with coverage, both the dimer and backbond states have undergone little changes. This indicates that the Ba adsorbate affects only the topmost silicon layer. A spectral shift as a whole towards greater binding energy is related to the band-bending shift. At $\Delta\phi = -2.08$ eV in association with 0.9

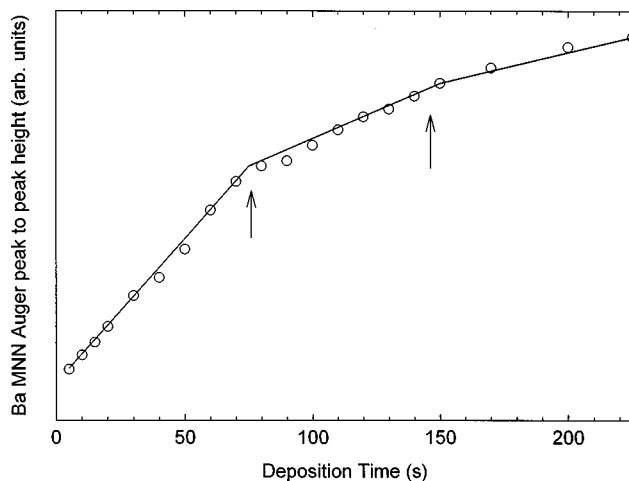


FIG. 1. The variation of the Ba *MNN* (56 eV) Auger peak-to-peak height during Ba deposition on the Si(001)2×1 surface at room temperature. Two break points are observed at about 75 and 150 s.

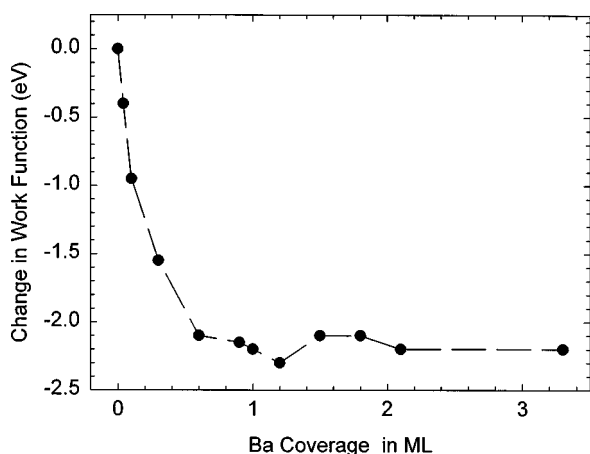


FIG. 2. The changes in the work function of Ba on Si(001)2 \times 1.

ML, however, a structure bulges up apparently at about 2.7 eV, and gets stronger with further deposition. It even enhances in intensity in the annealed spectrum. As will be shown later in the Si 2*p* core-level spectra, the formation of monosilicide starts to occur right from this coverage. Thus, the intense structure at 2.7 eV is attributed to the Ba-Si bonding state of that silicide.

Figure 4 exhibits the evolution of both the Si 2*p* and Ba 4*d* core-level spectra taken at $h\nu=130$ eV in normal emission for different Ba coverage. All spectra are normalized to the mesh current, and the Ba thickness in units of ML is shown on the right-hand side of the spectrum. As shown in Fig. 4, the ML-Ba spectrum moves as a whole towards higher binding energy by 0.46 eV. This direction of shift is similar to that in the saturated K and Na coverage, but certainly opposite to that in the saturated Cs coverage.⁵ Upon further deposition, the Si 2*p* core decreases gradually in intensity with coverage, and is vaguely seen at 5.7 ML. This phenomenon disagrees with the previous report that demonstrated high emission from the silicon substrate even at 10 ML of Ba thickness.⁹

The core-level line shape changes considerably during the interface formation. Figure 5 magnifies the Si 2*p* core-level spectra in great clarity. As can be seen in Fig. 5, the Ba adsorption broadens the vicinity of the valley between the central and the highest-binding-energy peaks, as well as the lowest-binding-energy peak, S_u . The latter structure has been attributed as emission from the up atoms in asymmetric dimers.¹⁸ The continued deposition does not entirely diminish the S_u component, but introduces a new component S at 0.9 ML. This S component differs from the S_u component in the clean spectrum both in line shape and surface core-level shift (SCLS). This indicates that the silicon surface atoms interfaced with the Ba adatoms now have a new atomic geometry.

Near the completion of one ML Ba, a new component, N_1 , starts to appear on the low-binding-energy side of the S component. Upon further deposition near to 2 ML, a second new component, N_2 , shows up even in a lower energy than the N_1 component. Both of them increase in intensity with increasing coverage. In a thick film, they remain rather strong, while other Si components reduce greatly in intensity. Hence, it is suggested that they be from the Si atoms

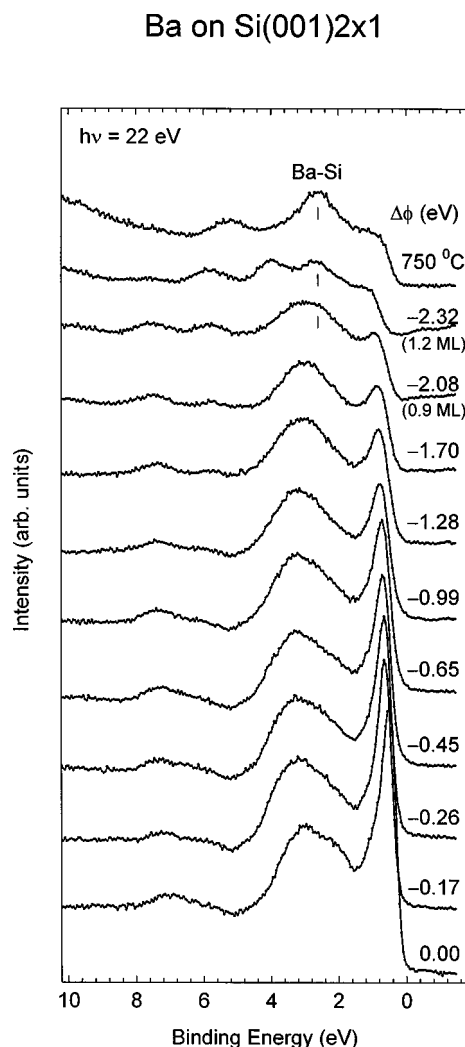


FIG. 3. Valence-band photoemission spectra taken at $h\nu=22$ eV in normal emission for different Ba coverage on a clean Si(001)2 \times 1 surface.

having diffused into and bonded with the Ba overlayer.

A fit to the Si 2*p* core-level spectra is exhibited in Fig. 6, where the spectra are normalized to a constant height in order to see clearly the evolution of each component. The raw and fitted data are plotted in dotted and line curves, respectively. The model function in a fit to the clean Si 2*p* core-level spectrum includes five Voigt-like spin-orbit-splitting states, denoted as B , S_u , C , SS , and S_d , and two Gaussian-like loss structures.¹⁹ The background function is represented by a power-law function. As to the 0.9- and 1.2-ML spectra, they are decomposed into six spin-orbit-splitting states, labeled as B , S , C , SS , S_d , and N_1 , and a loss structure, P . Components C and S_d were excluded in a fit to the 1.8-ML spectrum. For the 2.1-ML spectrum, an N_2 component was added, in addition to components B , S , SS , N_1 , and P . As a result, the spin-orbit splitting, the branching ratio, and the Lorentzian width are 606 ± 5 , 0.48 ± 0.02 , and 76 ± 14 meV, respectively.

For the clean spectrum, the SCLS of the S_u , S_d , C , and SS components is resolved at -497 , $+270$, -200 , and $+160$ meV, respectively. Components S_u and S_d are emission from the up and down atom in a dimer, respectively. The SS component denotes the atoms in the subsurface layer beneath the

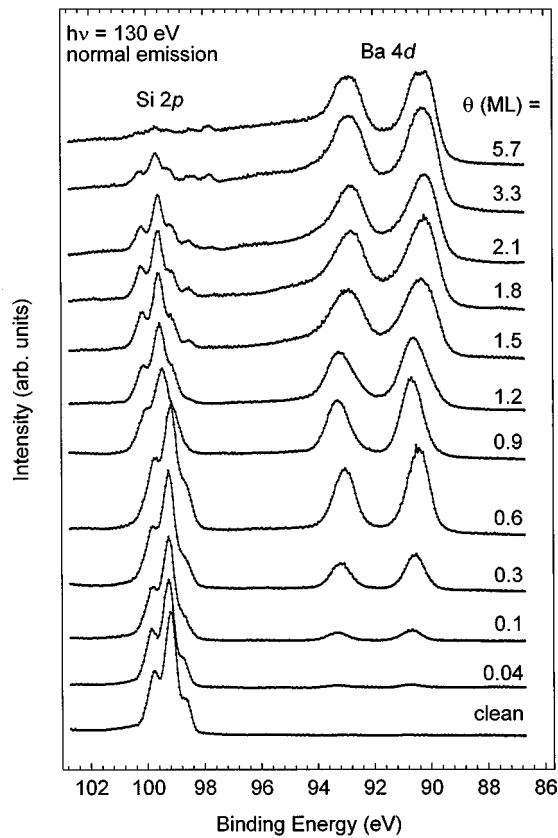


FIG. 4. Si 2*p* and Ba 4*d* core-level photoemission spectra taken at $h\nu=130$ eV in normal emission for different Ba coverage on a clean Si(001) 2×1 surface.

dimerized layer. The two loss structures are resolved at +1.3 and +1.7 eV. At 0.9-ML coverage, the SCLS of the *S* component is -404 meV. The N_1 component first has a SCLS of -0.78 eV at 0.9 ML, but gradually moves to -1.0 eV at 1.8 ML and above. The SCLS of the N_2 component is -1.84 eV. For a comparison, the Ca-induced SCLS is -0.65 eV.¹⁶ The electronegativity difference $\Delta\chi$ of Ba and Si and of Ca and Si is about -0.9 and -0.8 , respectively. If a linear slope of the SCLS versus $\Delta\chi$ is assumed, then the Ba-Si system has 5% deviation, compared to a near 20% deviation in the Ca-Si system.

In the recent report of the potassium adsorption on Si(001) 2×1 ,^{4,6,20} Chao *et al.* have shown that at saturation coverage, the intensity of the alkali-induced surface component is approximately twice that of the S_u component. In assistance with other experimental evidence, they then concluded that the dimers have become symmetric upon K adsorption. In the present Ba/Si(001) 2×1 system, not only the line shape of the Si 2*p* core-level spectrum at one ML resembles closely that in the AM/Si(001) 2×1 system, but the evolution of the *S* component is similar to that of the alkali-induced surface component. It is thus strongly suggested that the surface asymmetric dimers have become symmetric when the silicon surface has been covered with one Ba monolayer.

The *C* component that represents the valley structure between the S_u and *B* components of the uncovered spectrum must remain in the model function for a fit to the spectra corresponding to 0.9- and 1.2-ML coverage. In the

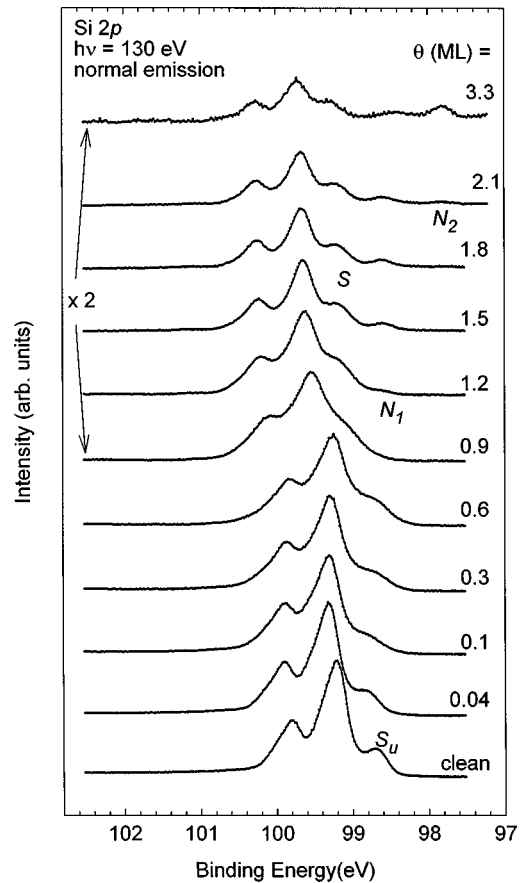


FIG. 5. Si 2*p* core-level photoemission spectra taken at $h\nu=130$ eV in normal emission for different Ba coverage on a clean Si(001) 2×1 surface.

AM/Si(001) 2×1 systems there exists a similar component, which has been postulated as emission from the third layer. In the present study, however, the *C* component remains rather strong near ML coverage, which makes that assignment questionable. With the mean free path at the present excitation energy being about 3.2 Å, emission from the third layer should be greatly diminished, considering the large atomic size of the adsorbate and the long vertical distance from that layer. Furthermore, the lack of an intensity oscillation with photon energies (not shown) renders the *C* component unlikely from the third-layer atoms. In the fit, the summation over the fractional areas of the *S* and N_1 components at 1.8 ML and that of the *S*, N_1 , and N_2 components at 2.1 ML are about the same as that of the S_u , *C*, and S_d components in the clean spectrum. This then suggests that the *C* component is surface-related emission. In the recent STM report of a clean Si(001) 2×1 surface at 6 K temperature, the symmetric dimers are clearly imaged.²¹ Although the high flip-flop rate of the dimers hinders the STM from revealing directly the image of the symmetric dimers at room temperature, their existence is certainly not unexpected. Recently, a theoretical calculation predicts that the SCLS of the atoms in a symmetric dimer is about -0.24 eV,²² a value with which the SCLS of the *C* component is in good agreement. Furthermore, the K-reverted dimers oriented symmetrically have revealed a negative SCLS.⁴ With all these evidences, we therefore believe that the *C* component is originated from the surface dimers in symmetric orientation.

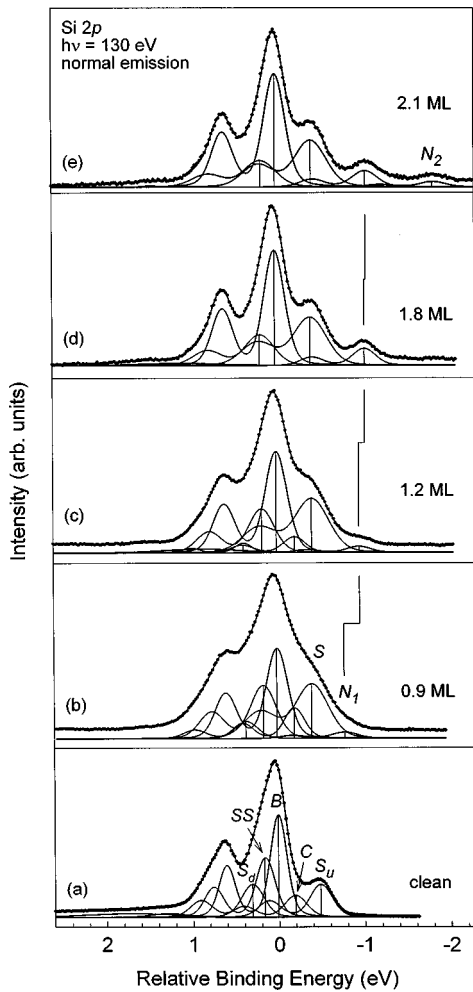


FIG. 6. Decomposed Si 2*p* core-level photoemission spectra taken at $h\nu=130$ eV in normal emission for (a) clean Si(001) 2×1 , (b) 0.9 ML, (c) 1.2 ML, (d) 1.8 ML, and (e) 2.1 ML Ba on a clean Si(001) 2×1 surface.

The reason for the minor change of the *C* component upon Ba adsorption is due to the fact that the asymmetric dimer has lower total energy than the symmetric dimer, thus making Ba atoms less preferable adsorbed on the latter. Above 1 ML, however, Ba starts to adsorb on the symmetric dimers, thereby reducing the *C* component. Further deposition ultimately makes it merged into the *S* component.

As shown in Fig. 6, the binding energy of the *S* component is -195 meV lower than that of the *C* component. This indicates that the dimers associated with component *S* must have excess charge from component *C*. The excess charge could be due to orbital hybridization or to charge transfer from the Ba adsorbate. However, the behavior of the Ba 4*d* core-level spectra denies the latter effect. See below.

Figure 7 shows the fitted results of the Ba 4*d* core-level spectra. One spin-orbit splitting state is enough to represent the line shape when the thickness is below 0.9 ML. Above that, however, the increased spectral broadening and line asymmetry require a second component for a proper representation of the line shape. At 2.1 ML, a small overlayer plasmon loss, *P*, is needed in the model function, as in the case of Cs/Si(001) 2×1 surface.⁵ The singularity index α is included for each spectrum for a proper fit. Its value is zero

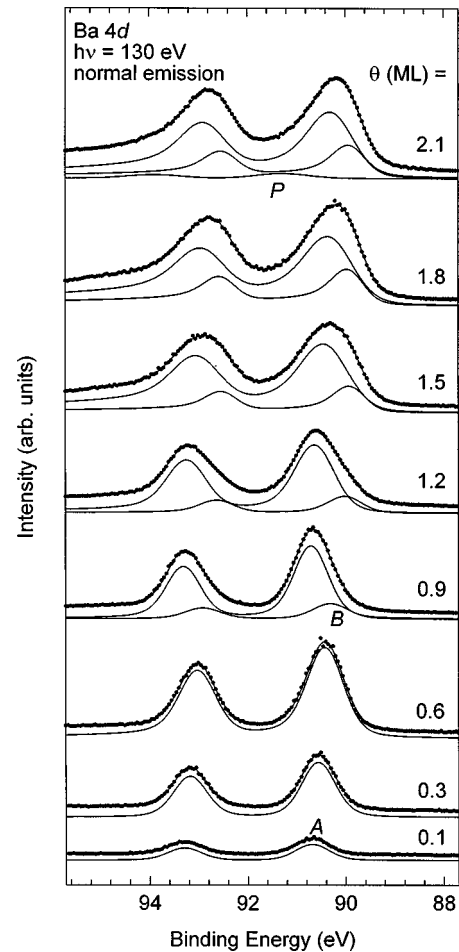


FIG. 7. Decomposed Ba 4*d* core-level photoemission spectra taken at $h\nu=130$ eV in normal emission for different Ba coverage on a clean Si(001) 2×1 surface.

for 0.1 ML, but goes up to 0.06 for 0.3, 0.9, and 1.2 ML, and to 0.2 above 1.5 ML of thickness. In thick coverage the Ba overlayer behaves as metallic Ba, thus giving larger α . As a result, the spin-orbit splitting, branching ratio, and Lorentzian width are 2.61 eV, 0.71 ± 0.03 , and 0.21 ± 0.04 eV, respectively.

The 4*d*_{5/2} core level of the *A* component shows initially at 90.65 eV at 0.1 ML, but gradually moves to 90.30 eV at 1.8 ML. Above that, it is fixed without further movement. A second low-energy component *B* does not appear until 0.9 ML of Ba coverage. Its intensity increases with increasing coverage, but is always smaller than that of component *A*. The energy separation between these two components is 0.6 eV near 1 ML, but reduces to 0.35 eV near 2 ML. In the Cs/Si(100) 2×1 system,⁵ in contrast, the second component of the Cs 4*d* core levels appears in a higher binding energy than the first component. Further, it is initiated in the submonolayer region and grows in intensity with coverage. At 1 ML, the second component has the same strength as the first component. Consequently, each component was assumed to occupy half of the Si(001) double layer. In the present Ba/Si(100) 2×1 system, the strength of the *B* component never exceeds that of the *A* component. Furthermore, it appears only when the Ba thickness is near ML coverage. Thus, the double-layer model is not feasible to the Ba/Si(100) 2×1 system.

Barium has a unique property that is not found in other elements; that is, the photoexcited oxidization state always appears in a *lower* binding energy than the clean state.²³ The phenomenon is attributed to the admixture of the $5d$ orbital in the conduction band, which occurred either in the initial or the final state. Moreover, the loss of the $6s^2$ electrons in Ba compounds increases the negative core-level shift of the oxidization states, since the empty $5d$ states are now energetically favorable to be filled. We then can apply this unique property to the Ba-Si interaction, with an expectation that the Ba cores would appear in low binding energy, provided that the $6s$ electron is lost in the interaction. Hence, the low binding energy of the B component suggests that the corresponding Ba atoms have donated their $6s$ electrons to silicon. This strong interaction then results in the formation of a silicide. The silicide formation then gives rise to the appearance of the N_1 and N_2 components in the Si $2p$ core-level spectra and the 2.7-eV bonding state in the valence-band spectra. As in the case of Ca,¹⁶ the N_1 and N_2 components are attributed to the Si atoms bonding to one and two Ba ligands, respectively. On the other hand, the high binding energy of the A component indicates that the Ba atoms that interfaced with the Si surface remain neutral. Thus, the previous conclusion of an ionic interaction due to the charge transfer is denied.^{10,11,13} Instead, the polarized model is more appropriate for the Ba/Si system.²⁴

The present finding of Ba-silicides formation at room temperature is in great contrast to all the previous reports, which had them shown only in an annealed film.^{8,10,11,13} We have taken a Si $2p$ core-level spectrum right after an Auger scan, during which the pressure was temporarily up to 8×10^{-10} Torr. In that spectrum, neither the N_1 nor the N_2 component appears. In other words, a slight gas residue could stop the formation of Ba silicides. As one closely examines the previous work,^{8,9,25} the uncovered Si $2p$ core-level spectrum fails to show strong surface emission.

The fact that the N_1 component first appears at near 1 ML indicates that a threshold thickness is needed for the formation of a silicide. This is because in the submonolayer region, the Ba adatoms bond directly with the Si dangling bonds, and the partial ionic bonding causes a polarization in the interface. After the dangling bonds are passivated, the excess

Ba breaks some of the dimer bonds. The break-off Si atoms then diffuse into the Ba overlayer and form a silicide. Any impurity residue such as carbon or oxygen, which bonds strongly with Si, certainly prohibits this reaction from happening. Note that the reaction occurs only on the surface without affecting the subsurface layer, since the SS component persists at the saturated coverage.

In the saturated AM/Si(001) 2×1 systems,^{4,5} the dimers remain asymmetric upon Cs adsorption, but become symmetric upon K adsorption. The dimer reversion is also found in the Sb/Si(001) 2×1 system.²⁶ The difference was claimed to be a weaker interaction between Cs and Si than between K and Si. The thermal desorption spectroscopy (TDS) has reached a similar conclusion, namely that the desorption temperatures are observed at about 470 and 600 K for the Cs/Si(001) (Ref. 27) and the K/Si(001) (Ref. 28) systems, respectively. In the ML Ba/Si(001) 2×1 system, the TDS gives rise to a desorption peak at about 1100 K,¹³ suggesting that the Si surface bonds stronger with the Ba adlayer than with the AM adlayer. The Ba adsorption has demonstrated the reversion of asymmetric dimers, which is absent in the Cs adsorption. This is somewhat surprising, considering that the Ba adsorbate in many respects behaves in the same way as the Cs adsorbate.⁷ Based on the fact of high desorption temperature of K and Ba, the reversion of the dimers must then be related to their strong electronic interaction with Si. In other words, the reversion is mainly a result of an electronic effect, not a chemical effect.

In summary, we have studied the Ba/Si(001) 2×1 interface using high-resolution synchrotron radiation photoemission. The maximum drop in work function upon Ba adsorption is ~ 2.3 eV. In submonolayer region, the dimer asymmetry is preserved and the Ba atoms interact mainly with the dangling bonds on the dimerized atoms. Above 1 ML, the dimers become symmetric. In the meantime, the first monosilicide starts to form. Upon further deposition to approximately 2 ML, the second disilicide appears.

This project was sponsored by the National Science Council under Contract No. NSC-86-2613-M-213-006. We thank Dr. G. K. Wertheim for allowing us to use his curve-fitting program.

*Present address: Department of Mathematics and Science Education, National Taitung Teacher College, Taitung, Taiwan, Republic of China.

[†]Author to whom correspondence should be addressed. Fax: +886 3 578 9816. Electronic address: pi@alpha1.ssrc.gov.tw

¹Y. Enta, T. Kinoshita, S. Suzuki, and S. Kono, Phys. Rev. B **39**, 1125 (1989).

²L. S. O. Johansson and B. Reihl, Phys. Rev. Lett. **67**, 2191 (1991).

³T. M. Grehk, L. S. O. Johansson, S. M. Gray, M. Johansson, and A. S. Flodström, Phys. Rev. B **52**, 16 593 (1995).

⁴Y.-C. Chao, L. S. O. Johansson, C. J. Karlsson, E. Landemark, and R. I. G. Uhrberg, Phys. Rev. B **52**, 2579 (1995).

⁵Y.-C. Chao, L. S. O. Johansson, and R. I. G. Uhrberg, Phys. Rev. B **54**, 5901 (1996).

⁶Y.-C. Chao, L. S. O. Johansson, and R. I. G. Uhrberg, Phys. Rev. B **55**, 7198 (1997).

⁷T.-W. Pi, I.-H. Hong, C.-P. Cheng, and R.-T. Wu, Surf. Rev. Lett. **4**, 1197 (1997).

⁸P. J. W. Weijts, J. C. Fuggle, and P. A. M. v. d. Heide, Surf. Sci. **260**, 97 (1992).

⁹P. J. W. Weijts, J. F. v. Acker, J. C. Fuggle, P. A. M. v. d. Heide, H. Haak, and K. Horn, Surf. Sci. **260**, 102 (1992).

¹⁰T. Urano, K. Tamiya, K. Ojima, S. Hongo, and T. Kanaji, Surf. Sci. **357**, 459 (1996).

¹¹D. Vlachos, M. Kamaratos, and C. Papageorgopoulos, Solid State Commun. **90**, 175 (1994).

¹²W. C. Fan and A. Ignatiev, Surf. Sci. **253**, 297 (1991).

¹³S. Hongo, K. Ojima, S. Taniguchi, T. Urano, and T. Kanaji, Appl. Surf. Sci. **82/83**, 537 (1994).

- ¹⁴T.-W. Pi, C.-H. Cheng, I.-H. Hong, M.-H. Ko, and R.-T. Wu, *Surf. Rev. Lett.* **5**, 101 (1998).
- ¹⁵A. Ishizaka and Y. Shiraki, *J. Electrochem. Soc.* **133**, 666 (1986).
- ¹⁶F. J. Himpsel, B. S. Meyerson, F. R. McFeely, J. F. Morar, A. Taleb-Ibrahimi, and J. A. Yarmoff, in *Photoemission and Adsorption Spectroscopy of Solids and Interfaces with Synchrotron Radiation*, edited by M. Campagna and R. Rosei (North-Holland, Amsterdam, 1990), p. 203.
- ¹⁷R. J. Gashman and E. Bassal, *Phys. Rev.* **55**, 63 (1939).
- ¹⁸E. Landemark, C. J. Karlsson, Y.-C. Chao, and R. I. G. Uhrberg, *Phys. Rev. Lett.* **69**, 1588 (1992).
- ¹⁹L. Gavioli, M. G. Betti, A. Cricenti, and C. Mariani, *J. Electron Spectrosc. Relat. Phenom.* **76**, 541 (1995).
- ²⁰Y.-C. Chao, L. S. O. Johansson, and R. I. G. Uhrberg, *Surf. Sci.* **372**, 64 (1997).
- ²¹H. Shigekawa, K. Hata, K. Miyake, M. Ishida, and S. Ozawa, *Phys. Rev. B* **55**, 15 448 (1997).
- ²²M. Rohlfiing, P. Krüger, and J. Pollmann, *Phys. Rev. B* **56**, 2191 (1997).
- ²³E. Wimmer, A. J. Freeman, J. R. Hiskes, and A. M. Karo, *Phys. Rev. B* **28**, 3074 (1983).
- ²⁴D. M. Riffe, G. K. Wertheim, J. E. Rowe, and P. H. Citrin, *Phys. Rev. B* **45**, 3532 (1992).
- ²⁵A. Mesarwi and A. Ignatiev, *J. Vac. Sci. Technol. A* **9**, 2264 (1991).
- ²⁶J. R. Power, T. Farrell, P. Gerber, S. Chandola, P. Weightman, and J. F. McGilp, *Surf. Sci.* **372**, 83 (1997).
- ²⁷C. A. Papageorgopoulos and M. Kamaratos, *Surf. Sci.* **221**, 263 (1989).
- ²⁸S. Tanaka, N. Takagi, N. Minami, and M. Nishijima, *Phys. Rev. B* **42**, 1868 (1990).